Consequences of cathepsin C inactivation for membrane exposure of proteinase 3, the target antigen in autoimmune vasculitis

Seren, Seda; Rashed Abouzaid, Maha; Eulenberg-Gustavus, Claudia; Hirschfeld, Josefine; Nasr Soliman, Hala; Jerke, Uwe; N'Guessan, Koffi; Dallet-Choisy, Sandrine; Lesner, Adam; Lauritzen, Conni; Schacher, Beate; Eickholz, Peter; Nagy, Nikoletta; Szell, Marta; Croix, Cécile; Viaud-Massuard, Marie-Claude; Al Farraj Aldosari, Abdullah; Ragunatha, Shivanna; Ibrahim Mostafa, Mostafa; Giampieri, Francesca

DOI:
10.1074/jbc.RA118.001922

Document Version
Peer reviewed version

Citation for published version (Harvard):
Seren, S, Rashed Abouzaid, M, Eulenberg-Gustavus, C, Hirschfeld, J, Nasr Soliman, H, Jerke, U, N'Guessan, K, Dallet-Choisy, S, Lesner, A, Lauritzen, C, Schacher, B, Eickholz, P, Nagy, N, Szell, M, Croix, C, Viaud-Massuard, M-C, Al Farraj Aldosari, A, Ragunatha, S, Ibrahim Mostafa, M, Giampieri, F, Battino, M, Cornillier, H, Lorette, G, Stephan, J-L, Goizet, C, Pedersen, J, Gauthier, F, Jenne, DE, Marchand-Adam, S, Chapple, IL, Kettritz, R & Korkmaz, B 2018, 'Consequences of cathepsin C inactivation for membrane exposure of proteinase 3, the target antigen in autoimmune vasculitis', *Journal of Biological Chemistry*, vol. 293, no. 32, pp. 12415-12428. https://doi.org/10.1074/jbc.RA118.001922

Consequences of cathepsin C inactivation on membrane expression of proteinase 3, the target antigen in autoimmune vasculitis

Seda Seren[1], Maha Rashed Abouzaid[2#], Claudia Eulenberg-Gustavus[3#], Josefine Hirschfeld[4#], Hala Soliman[5], Uwe Jerke[3], Koffi N'Guessan[1], Sandrine Dallet-Choisy[1], Adam Lesner[6], Conni Lauritzen[7], Beate Schacher[8], Peter Eickholz[8], Nikoletta Nagy[9], Marta Szell[9], Cécile Croix[10], Marie-Claude Viaud-Massuard[10], Abdullah Al Farraj Aldosari[11], Shivanna Ragunatha[12], Mostafa Ibrahim Mostafa[2], Francesca Giampieri[13], Maurizio Battino[13], Hélène Cornillier[14], Gérard Lorette[15], Jean-Louis Stephan[16], Cyril Goizet[17], John Pedersen[7], Francis Gauthier[1], Dieter E. Jenne[18], Sylvain Marchand-Adam[1], Iain L. Chapple[4], Ralph Kettritz[3,19] and Brice Korkmaz[1*]

[#] The authors contributed equally to this work

Running title: Cathepsin C inactivation and membrane-bound proteinase 3

*To whom correspondence should be addressed: Brice Korkmaz, INSERM U-1100 "Centre d'Etude des Pathologies Respiratoires (CEPR)",Université François Rabelais, Faculté de Médecine, 10 Bld. Tonnellé, 37032, Tours, France; e-mail: brice.korkmaz@inserm.fr; Tel: 0033 2 47 36 63 86

[1]INSERM U-1100, "Centre d'Etude des Pathologies Respiratoires" and Université François Rabelais, Tours, France
[2]Department of Oro-Dental Genetics, National Research Centre, Cairo, Egypt
[3]Experimental and Clinical Research Center, Charité und Max-Delbrück-Centrum für Molekulare Medizin in der Helmholtz-Gemeinschaft (MDC), Berlin, Germany
[4]Institute of Clinical Sciences, College of Medical and Dental Sciences, Periodontal Reseaech Group, University of Birmingham, and Birmingham Community Health Trust, Edgbaston, Birmingham, UK
[5]Department of Clinical Genetics, National Research Centre, Egypt
[6] Faculty of Chemistry, University of Gdansk, Poland
[7]Unizyme Laboratories A/S, Hörsholm, Denmark
[8]Department of Periodontology, Johann Wolfgang Goethe-University Frankfurt, Frankfurt, Germany
[9]Department of Medical Genetics, University of Szeged, Szeged, Hungary
[10]UMR-CNRS 7292 "Génétique, Immunothérapie, Chimie et Cancer" and Université François Rabelais, Tours, France
[11]Department of Prosthetic, College of Dentistry, King Saud University, Riyadh, Kingdom of Saudi Arabia
[12]Department of Dermatology, Venereology, and Leprosy, ESIC Medical College and PGIMSR Rajajinagar, Bengaluru, Karnataka, India
[13]Deptment Clinical Sciences, Università Politecnica delle Marche, Ancona, Italy
[14]Service de Dermatologie, Centre Hospitalier Universitaire de Tours, Université François Rabelais, Tours, France.
[15]UMR-INRA1282 « Laboratoire de Virologie et Immunologie Moléculaires », Université François Rabelais, Tours, France
[16]Service d'Hématologie Immunologie et Rhumatologie Pédiatrique, Centre Hospitalier Universitaire de Saint-Etienne, Saint-Priest-en-Jarez, France
[17]INSERM-U1211, Neuropediatric and Neurogenetic department, MRGM laboratory, Pellegrin Hospital and University, Bordeaux, France
[18]Comprehensive Pneumology Center, Institute of Lung Biology and Disease, German Center for Lung Research (DZL), Munich and Max Planck Institute of Neurobiology, Planegg-Martinsried, Germany

[19]Nephrology and Intensive Care Medicine, Charité-Universitätsmedizin, Berlin, Germany

Keywords: proteinase 3, cathepsin C, neutrophil, granulomatosis with polyangiitis, Papillon-Lefèvre syndrome

ABSTRACT

Membrane-bound proteinase 3 ($PR3^m$) is the main target antigen of anti-neutrophil cytoplasmic autoantibodies (ANCA) in granulomatosis with polyangiitis (GPA), a systemic small-vessel vasculitis. Binding of ANCA to $PR3^m$ triggers neutrophil activation with the secretion of enzymatically active PR3 and related neutrophil serine proteases, thereby contributing to vascular damage. PR3 and related proteases are activated from proforms by the lysosomal cysteine protease cathepsin C (CatC) during neutrophil maturation. We hypothesized that pharmacological inhibition of CatC provides an effective measure to reduce $PR3^m$ and has therefore implications as a novel therapeutic approach in GPA. We first studied PR3 in neutrophils from 21 patients with Papillon-Lefèvre syndrome (PLS), a genetic form of CatC deficiency. PLS neutrophil lysates showed a largely reduced, but still detectable (0.5-4%) PR3 activity when compared to healthy control cells. Despite extremely low levels of cellular PR3, the amount of constitutive $PR3^m$ expressed on the surface of quiescent neutrophils, and the typical bimodal membrane distribution pattern, was similar to what was observed in healthy neutrophils. However, following cell activation, there was no significant increase in the total amount of $PR3^m$ on PLS neutrophils, whereas the total amount of $PR3^m$ on healthy neutrophils was significantly increased. We then explored the effect of pharmacological CatC inhibition on PR3 expression in normal neutrophils using a potent cell permeable CatC inhibitor and a $CD34^+$ hematopoietic stem cell model. Human $CD34^+$ hematopoietic stem cells were treated with the inhibitor during neutrophil differentiation over 10 days. We observed strong reductions in $PR3^m$, cellular PR3 protein and proteolytic PR3 activity whereas neutrophil differentiation was not compromised.

Granulomatosis with polyangiitis (GPA) is a systemic small-vessel vasculitis most commonly affecting the upper and lower respiratory tract and kidneys (1,2). The main target autoantigen in GPA is the neutrophil serine protease (NSP) proteinase 3 (PR3) (EC 3.4.21.76) (3,4). GPA patients develop anti-neutrophil cytoplasmic autoantibodies to PR3 (PR3-ANCA) that bind to membrane-bound PR3 ($PR3^m$) on the neutrophil surface (5,6). The membrane expression of PR3 is mediated by a hydrophobic patch at the protease surface, which is not conserved in other related NSPs, such as human neutrophil elastase (HNE), cathepsin G (CG) and neutrophil serine protease 4 NSP-4 (7-9). Binding of PR3-ANCA to $PR3^m$ on cytokine-primed neutrophils induces cell activation resulting in neutrophil extracellular traps (NETs) production, and in granule protein and superoxide release (10,11). Secreted active proteases, including PR3 and related NSPs, exert proteolytic activity on endothelial cells thereby contributing to vascular necrosis (5,12). NETs are known to be directly implicated in ANCA induction as well as endothelial damage (13). There is no treatment for GPA that is based on disease-specific mechanisms and the current protocols involve combined administration of steroids with either cyclophosphamide or rituximab (14,15). These standard treatments are associated with toxicity highlighting the need to develop novel, more specific therapeutic strategies (16).

Cathepsin C (CatC) (EC 3.4.14.1), also known as dipeptidyl peptidase I, is a lysosomal amino peptidase belonging to the papain superfamily of cysteine peptidases (17). CatC catalyzes the cleavage of two residues from the N-termini of peptides and proteins. CatC, which is ubiquitously expressed in mammals is considered to be a major intracellular processing enzyme. High concentrations of CatC are detected in immune defense cells including neutrophils, mast cells, lymphocytes and macrophages. CatC is the physiological activator of several immune cell-associated serine proteases such as NSPs (18,19). NSPs are synthetized as inactive zymogens containing a di-propeptide in the myeloblast/promyelocyte stage in the bone marrow (8,20). The proforms mature in this very early developmental stage, induced by CatC, through the cleavage of the N-terminal di-propeptide. The cleavage of the di-propeptide by CatC results in a re-orientation

and remodeling of three surface loops within the activation domain of the protein and renders the S1 pocket of the active-site accessible to substrates (21). After processing, the active proteases are stored in cytoplasmic granules.

CatC is synthetized as a 60-kDa single chain pro-form containing an exclusion domain, a propeptide, a heavy chain and a light chain (22). Pro-CatC which is a dimer, can be efficiently activated by proteolysis with CatL and S *in vitro* (22). The initial cleavages liberate the propeptide from the catalytic region. Subsequently, a further cleavage occurs between the heavy chain and the light chain which form a papain-like structure (22,23). X-ray images of mature CatC structures revealed that the exclusion domain, the heavy chain and the light chain are held together by non-covalent interactions (17). Mature CatC is a tetramer formed by four identical monomers with their active site clefts fully solvent exposed. The presence of the exclusion domain blocks the active site beyond the S2 pocket and it is responsible for the diaminopeptidase activity of CatC (17,24).

Loss of function mutations in the CatC gene (*CTSC*) results in Papillon-Lefèvre syndrome (PLS) (OMIM: 245000) (25,26), a rare autosomal recessive disease affecting 1 to 4 persons per million (27,28). PLS involves an aggressive pre-pubertal periodontitis, leading to complete tooth loss in adolescence and palmoplantar keratoderma. More than 75 mutations have been identified in PLS, with missense and nonsense mutations being the most frequent, but small deletions, insertions and splice site mutations have also been reported (29). The presumptive diagnosis of PLS can be made by clinical signs and symptoms, but confirmation requires *CTSC* sequencing. Analysis of urinary CatC in suspected patients can be also used as an early, simple and easy diagnostic test (30). Roberts *et al*. (31) demonstrated a variety of neutrophil defects in PLS patients, arising downstream of the failure to activate NSPs by CatC. These functional defects included failure to produce NETs, reduced chemotaxis and exaggerated cytokine and reactive oxygen species release. Pham *et al*. (19) also studied neutrophils from PLS patients and observed that the loss of CatC activity was associated with strong reduction in the proteolytic activity of NSPs. In addition, only very low protein amounts of PR3 and related NSPs were detected in PLS neutrophils (32-34). Thus, it is conceivable that mimicking the genetic situation in PLS neutrophils by pharmacological CatC inhibition in bone marrow precursor cells would provide an attractive therapeutic strategy in GPA to eliminate major PR3-related disease mechanisms, including the PR3-ANCA autoantigen itself. However, the effect of CatC inactivation on PR3 that is presented on the neutrophil surface where it becomes accessible to anti-PR3 antibodies is not known.

In this work, we investigated the consequences of CatC inactivation on membrane-expression of PR3. First, we quantified the residual proteolytic activity of CatC and PR3 in white blood cell (WBC) lysates or isolated neutrophils from PLS patients. Second, we studied the membrane-expression of PR3 on PLS neutrophils. Finally, we used a potent synthetic cell permeable nitrile inhibitor to evaluate the effect of pharmacological CatC inhibition on membrane-PR3 expression in normal neutrophils generated from human $CD34^+$ progenitor cells.

Results

CatC in blood cells from PLS patients

Blood samples were collected from 13 PLS patients from European, Asian and African countries. PLS diagnosis was firmly established by genetic testing. These patients carried either premature stop codon, missense, nonsense or frameshift mutations in their *CTSC* (**Table I**). Blood from 8 additional patients with clinically suspected PLS was obtained. These patients showed typical symptoms of early-onset periodontitis and hyperkeratosis (**Fig. 1A**). WBC lysates from these patients and from healthy controls differed by their protein profile as observed by SDS-PAGE (**Fig. 1B**). CatC activity was assayed in peripheral WBC lysates or in purified neutrophils using a CatC-selective FRET substrate in the presence or absence of the selective nitrile CatC inhibitor (L)-Thi-(L)-Phe-CN. Strong CatC activity was observed in control neutrophils and was completely abrogated by the specific CatC inhibitor. In contrast, we did not detect any CatC activity in samples, from genetically and clinically diagnosed PLS patients (**Table I** and **Fig. 1C**), nor any CatC protein in cell lysates from PLS patients using a specific anti-CatC Ab (**Fig. 1D**). CatC activity and the CatC antigen were also absent in the urine of all PLS patients, unlike healthy controls (**Fig. 1C, D**). Thus, the

CatC deficiency of all 7 patients was confirmed as described in (30) and the mutations were identified by *CTSC* gene sequencing for some of these patients (**supp.Fig. 2, Table I**). Once CatC deficiency was clearly established, we studied the fate of PR3 in samples from PLS patients.

Proteolytically active PR3 in blood cells from PLS patients

WB analysis of white blood cell or neutrophil lysates from PLS patients showed that low amounts of the PR3 antigen were still present in all PLS samples (**Fig. 2A** and **supp.Fig. 4A**). We checked that residual PR3 was enzymatically active by incubating PLS samples with purified exogenous alpha-1-proteinase inhibitor (α1PI) (35) and observing the appearance of an additional ~75 kDa band corresponding to the irreversible complex between active PR3 and its inhibitor (**Fig. 2B**). In contrast to mature PR3, inactive pro-PR3 did not form any irreversible complex with α1PI (**Fig. 3**). We confirmed the presence of proteolytically active PR3 in permeabilized PLS neutrophils using an activity-based probe ($Bt\text{-}PEG_{66}\text{-}PYDA(O\text{-}C_6H_4\text{-}4\text{-}Cl)_2$) selective for PR3 and a fluorescent streptavidin derivative to reveal the formation of irreversible complexes (**Fig. 2C)**. We also measured PR3 activity in supernatants of PLS cells activated with the A23187 calcium ionophore using ABZ-VAD(nor)VADYQ-EDDnp as a substrate (**Fig. 2D**). PR3 activity in PLS cell supernatants was about 1/20 that in controls cells and was almost totally abrogated by the PR3-specific inhibitor $Bt\text{-}PYDA^{P}(O\text{-}C_6H_4\text{-}4\text{-}Cl)_2$. We found that 10 to 20 times more cell lysate proteins from PLS patients (2.5 to 5 µg/well) as compared to healthy controls (0.25 to 0.5 µg/well), were required to achieve similar PR3 activity values. Enzymatic activities in PLS cells and healthy control cells, measured on ABZ-VAD(nor)VADYQ-EDDnp substrate, were almost completely inhibited by the PR3 inhibitor (**Fig. 4A, B, C)**. From these results, we estimated that blood cells of PLS patients contained from 0.5 to 4% of the PR3 activity in healthy controls cells (**Fig. 4D** and **Table I**). Marginal, but still detectable activity of CG was also observed in PLS samples using the appropriate selective FRET substrate (*data not show*). Next, we checked whether PR3 was present at the cell surface of PLS neutrophils.

Membrane surface expression of PR3 on PLS neutrophils

Since the membrane expression of PR3 depends on the activation status of neutrophils, we analyzed both quiescent neutrophils from two local patients (PLS 13 and PLS 14) 30 min after blood collection and neutrophils from foreign blood samples collected 24-72 h before the analysis and thus inevitably activated during shipping. As a control for the latter conditions, cells from either the parents or healthy individuals of the patient's country-of-origin were collected at the same time. The flow cytometry analysis of $PR3^{m}$ using anti-PR3 mAbs CLB12.8 showed that constitutive $PR3^{m}$ was present in significant amounts on quiescent PLS neutrophils and showed the typical bimodal pattern with low ($PR3^{m(low)}$) and high ($PR3^{m(high)}$) subsets. After cell activation with a calcium ionophore (A23187), we observed a single homogeneous PR3 population but no significant increase of the total amount of $PR3^{m}$ at the surface of PLS neutrophils whereas the bimodal pattern was conserved on control cells and the total amount of PR3 increased significantly (**Fig. 5**). We also found a single $PR3^{m}$-presenting neutrophil population in PLS cells that were spontaneously and inevitably activated during transit (experiments with cells from 9 different PLS patients, **Fig. 6** and **supp.Fig. 4**). The PR3 mean fluorescence intensity of these PLS neutrophils was 26 ± 8 % of the intensity found in controls. Thus, the absence of CatC in PLS patients affected constitutive PR3 expression at the surface of quiescent neutrophils only marginally but largely reduced the PR3 antigen exposure on the neutrophil surface of activated cells. Next, we assessed whether an early treatment of neutrophil precursor cells by a CatC inhibitor, would diminish $PR3^{m}$ expression, cellular PR3 amount and proteolytic activity.

Membrane surface expression of PR3 on neutrophils generated from human $CD34^{+}$ progenitor cells in the presence of a CatC inhibitor

We differentiated human $CD34^{+}$ HSC isolated from umbilical cord blood into neutrophils in the presence or absence of a potent cell permeable cyclopropyl nitrile CatC inhibitor (IcatC) (32). Expression of the neutrophil surface markers CD16, CD66b, and CD11b was assessed by flow cytometry during the 10 day differentiation period and confirmed

neutrophil differentiation (**Fig. 7A**). At day 10, a typical bimodal $PR3^m$ expression pattern was observed by flow cytometry with a $PR3^m$-positive neutrophil subset of approximately 30-40%. Importantly, CatC inhibition with the pharmacological compound IcatC did not affect neutrophil differentiation, but eliminated the bimodal $PR3^m$ expression pattern leaving only marginal $PR3^m$ amounts on the cell surface (**Fig. 7A**). The mean fluorescence intensity values for $PR3^m$ were reduced to 17±5 % by IcatC at day 10 ($p<0.01$). The analysis by immunoblotting of cell lysates of differentiated neutrophils, showed that the amount of PR3 protein was strongly reduced after treatment with the CatC inhibitor (**Fig. 7B**) and that residual PR3 was enzymatically inactive (**Fig. 7C**). Thus, inhibition of CatC in progenitor cells reduces both cellular and membrane PR3. This PR3 reduction was even stronger than that observed in neutrophils from PLS patients with genetic CatC deficiency.

Discussion

Neutrophils are key actors in the pathogenesis of ANCA-associated vasculitis (6). Neutrophil activation results in the production of NETs bearing PR3 (11). NETs-associated PR3 is presented to dendritic cells triggering the production of PR3-ANCA by B-cells (6). In addition, PR3 is the only NSP that is presented constitutively on the surface of circulating blood neutrophils and remains partly bound to the neutrophil surface following cell activation. These findings contribute to the important role of PR3 as the main target antigen in GPA and related vasculitis. Interaction of circulating PR3-ANCA with $PR3^m$ initiates the activation of circulating neutrophils and thus triggers necrotizing inflammation (6). Because neutrophils from PLS patients that lack CatC activity do not produce NETs (31,34) and contain only marginal levels of NSPs (19,33), it is reasonable to assume that blocking NETosis and/or eliminating PR3 by interfering with CatC activity pharmacologically would ultimately reduce vascular inflammation. Thus, *in vivo* inhibition of CatC by a synthetic cell permeable inhibitor that mimicks the conditions observed in PLS patients, could have therapeutic potential by reducing PR3-ANCA production, neutrophil activation, endothelial cell necrosis and inflammation. We have compared here the effects of genetic and pharmacological CatC inactivation on the fate of soluble PR3 and $PR3^m$.

Because CatC is pathologically inactivated by gene mutations in PLS patients, we first used WBC lysates from 21 PLS, 17 of these patients with established missense, frameshift or nonsense mutations, to investigate the fate of cellular and membrane PR3. As expected, we observed neither CatC activity nor immunoreactive CatC protein in PLS cell lysates irrespective of the underlying CatC mutations. It may be surprising that mutated CatC with a missense mutation was neither detected in cell lysates nor in the urine of PLS patients (30). However, our observation corroborates a previous report from the literature (34) and gives support to the conclusion that missense mutations in the *CTSC* gene abrogates the constitutive secretion of CatC and triggers its degradation in intra- or extra cellular compartments.

The loss of CatC activity in PLS patients was associated with a severe reduction in the activity and the amounts of NSPs (19,32-34). We also found that PR3 activity in PLS WBC lysates was strongly lowered to 1-4% of that in control lysates, but was still detectable. We employed several approaches to ensure that the measured proteolytic activity was indeed due to PR3. We used a highly sensitive and specific PR3 substrate, a specific PR3 inhibitor that totally abrogated the enzymatic activity, and finally, a selective PR3 activity-based probe to detect active PR3 in PLS neutrophils. The results clearly confirmed the presence of residual active PR3 in PLS neutrophils, suggesting that CatC is the main, but not the sole protease involved in the activation of pro-NSPs. This observation is consistent with data from Roberts *et al*. who demonstrated the presence of some LL37 in stimulated neutrophil supernatants from PLS patients, LL37 being a product of PR3 cleavage of human cathelicidin 18 (31).

We then investigated whether or not the unprocessed pro-PR3 was still present in PLS cell lysates. For this purpose, we exploited the property of α1PI to form irreversible complexes with proteolytically active PR3 but not with its proform. Following incubation of PLS cell lysates with α1PI, almost all immunoreactive PR3 formed irreversible complexes with the inhibitor suggesting that only residual mature PR3 was present in cell lysates. Having ensured that the absence of the pro-PR3 was not due to the cell lysis procedure, we conclude that most

of pro-PR3 was degraded very early in PLS neutrophil precursors. Our data are compatible with the notion that a small amount of the pro-PR3 can be early processed into an active protease by one or several aminopeptidase(s) other than CatC. These enzymes remain to be identified.

Human PR3 is expressed constitutively in a bimodal manner with two populations of neutrophils presenting either high ($PR3^{m(high)}$) or low ($PR3^{m(low)}$) amounts of the protease on their surface (36,37). The level of $PR3^m$ on resting neutrophils and the percentage of $PR3^m$ expressing neutrophils is stable over time for a given individual (5,37). In spite of the low PR3 level in PLS cell lysates, we observed that $PR3^m$ was present at the surface of resting PLS neutrophils showing a typical bimodal distribution similar to control neutrophils. This observation suggests that the expression of constitutive $PR3^m$ on resting neutrophils is independent of intracellular PR3 levels and remains stable even when CatC is inactive. Activating cells from PLS patients with the calcium ionophore A23187 resulted in a PR3 increase on the neutrophil surface but this increase was significantly smaller than that observed in control cells. Thus, the genetic inactivation of CatC results in a dramatic decrease of PR3 within intracellular granules but does not interfere with the constitutive expression of proteolytically inactive PR3 (38,39) at the surface of quiescent PLS neutrophils. This data suggests a different intracellular storage site and a different intracellular pathway for constitutive and induced $PR3^m$. Unexpectedly, and in contrast to control cells, no bimodal $PR3^m$ expression pattern was observed in activated PLS cells. This observation was made in both spontaneously activated cells during shipping and with a pharmacological compound. We have no obvious explanation for this finding at the moment.

We showed previously that a two-step amplification/differentiation protocol of human $CD34^+$ hematopoietic stem cells obtained from umbilical cord blood results in differentiated neutrophils (40). We used this model system to investigate the production and the fate of PR3 in the presence of a CatC nitrile inhibitor, IcatC (23). A subset of $PR3^m$-positive cells was detectable by flow cytometry at day10 whereas a second cell subset remained negative, consistent with a bimodal expression typically seen with blood neutrophils. Differentiation of $CD34^+$ HSC into neutrophils in the presence of the CatC inhibitor IcatC did not alter the expression of the neutrophil surface markers CD16b, CD66b and CD11b but resulted in strong reduction of intracellular and membrane PR3. Pharmacological CatC inhibition eliminated PR3 from normal neutrophils more effectively than mutated CatC in PLS neutrophils. It is conceivable that additional aminopeptidases exist in blood neutrophils that were absent in $CD34^+$ HCS-derived neutrophils or that the potent IcatC inhibitor inhibited CatC together with additional proteases involved in the activation of the pro-PR3. Our current observations in PLS cells and our recent work reporting the complete disappearance of HNE in bone marrow cells from healthy donors pulse-chased in presence of IcatC supports the latter hypothesis (32).

To conclude, we showed here that CatC is the major but not the unique pro-PR3 processing protease in neutrophils since low amounts of proteolytically active PR3 are still present in neutrophils of CatC deficient individuals. Treating $CD34^+$ hematopoietic stem cells with the CatC inhibitor ICatC resulted in an almost total absence of intracellular PR3 and $PR3^m$ in stem cells-derived neutrophils. The elimination of the PR3-ANCA target antigen supports the notion that pharmacological CatC inhibition provides an alternative therapeutic strategy for reducing neutrophil-mediated vascular inflammation in auto-immune vasculitis. We previously showed that a prolonged IcatC administration in the macaque resulted in an almost complete elimination of PR3 and NE (32). Unlike humans however, macaques do not display constitutive PR3 at the surface of their circulating neutrophils and therefore cannot be used as a relevant model of GPA. Only clinical studies in GPA patients will answer the question whether or not a CatC inhibitor may function as a PR3-ANCA antigen suppressor.

Experimental Procedures

Blood collection- Blood samples were collected from 21 PLS patients from European countries (Germany, the UK, Italy, France, Hungary), from Asian countries (India, Saudi Arabia) and from Egypt. The 13 healthy volunteers were from France, India, Italy, Saudi Arabia and Egypt. 2-15 mL peripheral blood

samples from healthy control donors and patients with PLS were collected into EDTA K2 preservative tubes by peripheral venipuncture. Samples were taken giving informed consent. Red blood cells lysis took place with 0.1 mM EDTA, 10 mM $KHCO_3$, 150 mM NH_4Cl and white cells pelleted with centrifugation for 5 min at 400 x g.

Blood neutrophil purification- Neutrophils were isolated by Percoll density centrifugation, employing two discontinuous gradients of 1.079 and 1.098, and purified by erythrocyte lysis (0.83% NH_4Cl containing 1% $KHCO_3$, 0.04% EDTA, and 0.25% BSA) previously described (31). Cells were then re-suspended in gPBS (phosphate-buffered saline) (1 mM glucose) and cations (1 mM $MgCl_2$, 1.5 mM $CaCl_2$). Cell viability was determined by Trypan blue dye exclusion (typically 98%) and cell purity by cytospin.

Differentiation of CD34$^+$ hematopoietic stem cells from umbilical cord blood into neutrophils- Umbilical cord blood samples were taken giving informed consent. Mononuclear cells were obtained from anti-coagulated cord blood by centrifugation over a LSM1077 (PAA, Pasching, Austria) gradient at 800 x g for 20 min. Cells were washed and stained using the CD34$^+$ progenitor isolation kit (Miltenyi, Bergisch-Gladbach, Germany) and sorted according to the manufacturer's instructions. CD34$^+$ cells were cultivated in stem span serum free medium (Cell Systems, St. Katharinen, Germany) supplemented with Penicillin/Streptomycin, 100 ng/mL SCF, 20 ng/ml TPO and 50 ng/mL FLT3-L (Peprotech, London, UK) for expansion. Neutrophil differentiation was performed in RPMI with 10% FCS, 10 ng/mL G-CSF (Peprotech), and either DMSO control or 1 µM IcatC. Medium was changed every other day. We PR3-phenotyped the neonatal neutrophils obtained from the freshly harvested umbilical cords by flow cytometry prior to the CD34$^+$ HSC isolation. We selected only cord blood where the neonatal neutrophils showed a clear bimodal membrane PR3 pattern.

Measurement of protease activities in cell lysates- WBC, purified blood neutrophils, CD34$^+$ or neutrophil-differentiated CD34$^+$ HSC were lysed in 50 mM HEPES buffer, 750 mM NaCl, 0.05% NP-40, pH 7.4. Soluble fractions were separated from cell debris by centrifugation at 10,000 x g for 10 min. Soluble fractions were concentrated by ultrafiltration (Vivaspin (filtration threshold 10 kDa)) in some experiments. Proteins were assayed with a bicinchoninic acid assay (BCA) (Thermo Fisher Scientific, Villebon sur Yvette, France).

The CatC activity in cell lysates was measured spectrofluorometrically (Spectra Max Gemini EM) at 420 nm with or without the nitrile inhibitor (L)-Thi-(L)-Phe-CN (23) (1 µM final, 20 min incubation at 37°C) using Thi-Ala(Mca)-Ser-Gly-Tyr(3-NO_2)-NH_2 (41) (20 µM final) as selective fluorescence resonance energy transfer (FRET) substrate in 50 mM sodium acetate, 30 mM NaCl, 1 mM EDTA, 2 mM DTT, pH 5.5 at 37°C. Mature human CatC was used as control (Unizyme Laboratories, Hørsholm, Denmark).

The PR3 activity in cell lysates was measured at 420 nm with or without the PR3 inhibitor Ac-PYDA^P(O-C_6H_6-4-Cl)$_2$ (42) (0.5 µM final, 20 min incubation at 37°C) using ABZ-VAD(nor)VADYQ-EDDnp (20 µM final, Genecust, Dudelange, Luxembourg) as a substrate in 50 mM HEPES buffer, 750 mM NaCl, 0.05% NP40, pH 7.4 at 37°C. The CatG activity was measured at 420 nm in 50 mM HEPES buffer, 100 mM NaCl, 0.05% NP-40, pH 7.4 at 37°C, in the presence or not of 2 µM antichymotrypsin, using ABZ-TPFSGQ-EDDnp (43) (20 µM final, Genecust, Dudelange, Luxembourg) as a substrate.

Western blotting- The pellet of purified blood neutrophils and WBC were directly lysed in SDS sample buffer (25 mM Tris (pH 7), 10% glycerol, 1% SDS, 10% 2-mercaptoethanol). The pellet of CD34$^+$ HSC or neutrophil-differentiated CD34$^+$ HSC were lysed in sample buffer (20 mM Tris (pH 8,8), 138 mM NaCl, 10% glycerol, 2 mM EDTA, 1%Triton-X-100, 1% NP-40 and protease inhibitor mix). The total protein concentration has been determined by the BCA (Thermo Fisher Scientific, Villebon sur Yvette, France) or Bradford (Bio-Rad, Hercules, USA) assay.

The proteins were separated on 10% or 12% SDS-polyacrylamide gel electrophoresis (SDS-PAGE) under reducing and denaturing conditions (7-50 µg of protein per lane). They were transferred to a nitrocellulose (Hybond)-Enhanced chemiluminescence (ECL) membrane at 4°C. Free sites on the membranes were blocked by incubation with 5% nonfat

dried milk in PBS, 0.1% Tween for 90 min at room temperature (RT). They were washed twice with PBS, Tween 0.1% and incubated overnight with a primary antibody (murine anti-human CatC antibody (Ab) directed against the heavy chain of CatC (Ab1, sc-747590) (1:1000, Santa Cruz Biotechnology, Heidelberg, Germany (30)), goat anti-human CatC (Ab2, EB11824) directed against the propeptide (1:1000, Everest Biotech, Oxfordshire, UK (30)), rabbit anti-PR3 Ab (ab133613) (1:1000, Abcam, Cambridge, UK) (23)), rabbit anti-myeloperoxydase (MPO) heavy chain (1:500, sc-16128-R, Santa Cruz Biotechnology, Heidelberg, Germany) followed by a specific secondary antibody (a sheep anti-mouse IgG secondary antibody (1:10000, A5906, Sigma-Aldrich), a goat anti-rabbit IgG secondary antibody (1:10000, A9169, Sigma-Aldrich)). Membranes were washed (3 x 10 min) with PBS, 0.1% Tween and the detection was performed by ECL system.

Flow cytometry- WBC from PLS patients or healthy controls were resuspended in PBS and a blocking step was performed with 5% bovine serum albumin (BSA), 2.5 mM EDTA in PBS for 15 min at 4°C. Or WBC were fixed with 2% paraformaldehyde and permeabilized with 0,5% Triton-X 100 in PBS and non-specific binding sites were blocked with 5% BSA. Flow cytometry analyses were performed using a MACSQuant analyzer (Miltenyi Biotec, Bergisch-Gladbach, Germany) and VenturiOne software (Applied Cytometry, Sheffield, United Kingdom). These analyses were performed using the following Abs: V450-conjugated CD14 (MφP9, 1:200), PE-conjugated CD3 (HIT3a, 1:200), PE-Cy™-conjugated CD11b (M1/70, 1:100), APC-conjugated CD16 (3G8, 1:200), APC-H7-conjugated CD45 (2D1, 1:200) (BD Biosciences, Le Pont de Claix, France), PerCP-Vio700-conjugated CD15 (VIMC6, 1:100) (Miltenyi Biotec, Bergisch-Gladbach, Germany), FITC-conjugated IgG1 (679.1Mc7, 1:20) (Dako, Hamburg, Germany), FITC-conjugated CD16 (DJ130c, 1:20) (Dako, Hamburg, Germany), FITC-conjugated CD18 (/E4, 1:20) (Beckmann Coulter, Krefeld, Germany), FITC-conjugated CD66b (80H3, 1:20) (Beckmann Coulter, Krefeld, Germany). The PR3 was labelled with the primary mouse mAb CLB12.8 (1:50) (Sanquin, Amsterdam, Netherlands) and the secondary antibody FITC-conjugated anti-mouse IgG (sc-2010, 1:100) (Santa Cruz Biotechnology, Heidelberg, Germany) or the secondary antibody FITC-conjugated IgG1 Fab_2 (DAK-GQ1, 5µg/mL) (Dako, Hamburg, Germany). Dead cells were stained with Viobility 405/520 Fixable Dye (1:200) (Miltenyi Biotec, Bergisch-Gladbach, Germany). The gating strategies used are described in **supp.Fig. 1**. The compensation was performed using VenturiOne software.

Genetic analysis-

Extraction of genomic DNA (salting out procedure): Peripheral blood samples were obtained from the patients and both parents (if available) after informed consent had been given according to NRC guidelines. Genomic DNAs were prepared as previously described by (44) with some additional modifications described by (45).

PCR amplification of *CTSC* gene exons: For analysis of *CTSC* mutations, eight different specific amplifications using *CTSC* gene specific primers carried out on the genomic DNA according to Toomes *et al*., (26), except for the newly developed primer pairs for exons 1 and the 5′ half of exon 7.

Exon No.	*Sequence of Forward Primer*
1	5′–TCTTCACCTCTTTTCTCAGC–3′
2	5′–GACTGTGCTCAAACTGGGTAG–3′
3	5′–GGGGCACATTTACTGTGAATG–3′
4	5′–GTACCACTTTCCACTTAGGCA–3′
5	5′–CCTAGCTAGTCTGGTAGCTG–3′
6	5′–CTCTGTGAGGCTTCAGATGTC–3′
7a	5′–CGGCTTCCTGGTAATTCTTC–3′
7b	5′–CAATGAAGCCCTGATCAAGC–3′
	Sequence of Reverse Primer
1	5′–GGTCCCCGAATCCAGTCAAG–3′
2	5′–CTACTAATCAGAAGAGGTTTCAG–3′
3	5′–CGTATGTCTCATTTGTAGCAAC–3′
4	5′–GGAGGATGGTATTCAGCATTC–3′
5	5′–GTATCCCCGAAATCCATCACA–3′
6	5′–CAACAGCCAGCTGCACACAG–3′
7a	5′–GTAGTGGAGGAAGTCATCATATAC–3′
7b	5′–CTTCTGAGATTGCTGCTGAAAG–3′

PCR was performed in a final volume of 25 µL containing ~ 100 ng genomic DNA, $MgCl_2$ (1.5 mM), dNTP mixture (0.2 mM), Taq DNA polymerase (2 U/µL), and 10 µM of each primer (MWG-BIOtech, Ebersberg, Germany).

The amplification conditions were as follows: 2 min at 95°C for one cycle, followed by 35 cycles of 30 s at 94°C, 30 s at the annealing temperature of the primers (53°C for exons 7a and 7b, 54.5°C for exon2, 55.2°C for exons 1 and 6, 56.6°C for exon 3, 57.2°C for

exon 4 and 58°C for exon 5), and 1 minute at 72°C in a thermal cycler (Agilent Technologies SureCycler 8800) (46). Five microliters aliquots of the PCR products were analyzed by 2% agarose gel electrophoresis.

Mutation analysis: PCR products were purified using the QIA Quick PCR Purification kit (Qiagene) followed by bidirectional sequenced using the ABI Prism Big Dye Terminator v3.1 Cycle Sequencing kit (Applied Biosystems) and the sequencing reaction products were separated on an ABI Prism 310 Genetic Analyzer (Applied Biosystems). Alignment of sequenced results used NCBI genomic sequence NG_008365.1 and reference cDNA sequence NM_000348.3 for result interpretation.

Acknowledgments: This work was supported by the **"**Ministère de l'Enseignement Supérieur et de la Recherche", the "Région Centre-Val de Loire" (Project BPCO-Lyse). This project has received funding from the *European Union's Horizon 2020 research and innovation programme* under grant agreement No 668036 (RELENT). Responsibility for the information and views set out in this study lies entirely with the authors. BK acknowledges the "Alexandre von Humboldt Foundation" for a short term institutional research training grant (2016, Comprehensive Pneumology Center, Munich). The authors thank Lise Vanderlynden (INSERM U-1100) for technical assistance.

Conflicts of interest: The authors declare no competing financial interests.

Authorship contributions: Brice Korkmaz supervised the work. Brice Korkmaz, Ralph Kettritz and Sylvain Marchand-Adam participated in the research design. Seda Seren, Maha Rashed Abouzaid, Claudia Eulenberg-Gustavus, Josefine Hirschfeld, Hala Soliman, Uwe Jerke, Koffi N'Guessan, Sandrine Dallet-Choisy, conducted the experiments. Brice Korkmaz, Ralph Kettritz, Iain Chapple, Sylvain Marchand-Adam, Dieter E. Jenne, Francis Gauthier performed data analyses. All other authors contributed samples or other essential material (chemical compounds, PLS bloods/urines). Brice Korkmaz and Ralph Kettritz wrote the manuscript. All authors contributed to the writing and revision processes of the manuscript.

References

1. Millet, A., Pederzoli-Ribeil, M., Guillevin, L., Witko-Sarsat, V., and Mouthon, L. (2013) Antineutrophil cytoplasmic antibody-associated vasculitides: is it time to split up the group? *Ann Rheum Dis* **72**, 1273-1279
2. Pagnoux, C. (2016) Updates in ANCA-associated vasculitis. *Eur J Rheumatol* **3**, 122-133
3. Jenne, D. E., Tschopp, J., Ludemann, J., Utecht, B., and Gross, W. L. (1990) Wegener's autoantigen decoded. *Nature* **346**, 520
4. Thieblemont, N., Wright, H. L., Edwards, S. W., and Witko-Sarsat, V. (2016) Human neutrophils in auto-immunity. *Semin Immunol* **28**, 159-173
5. Kettritz, R. (2016) Neutral serine proteases of neutrophils. *Immunol Rev* **273**, 232-248
6. Schonermarck, U., Csernok, E., and Gross, W. L. (2015) Pathogenesis of anti-neutrophil cytoplasmic antibody-associated vasculitis: challenges and solutions 2014. *Nephrol Dial Transplant* **30 Suppl 1**, i46-52
7. Korkmaz, B., Kuhl, A., Bayat, B., Santoso, S., and Jenne, D. E. (2008) A hydrophobic patch on proteinase 3, the target of autoantibodies in Wegener granulomatosis, mediates membrane binding via NB1 receptors. *J Biol Chem* **283**, 35976-35982
8. Korkmaz, B., Horwitz, M. S., Jenne, D. E., and Gauthier, F. (2010) Neutrophil elastase, proteinase 3, and cathepsin G as therapeutic targets in human diseases. *Pharmacol Rev* **62**, 726-759
9. Korkmaz, B., Moreau, T., and Gauthier, F. (2008) Neutrophil elastase, proteinase 3 and cathepsin G: physicochemical properties, activity and physiopathological functions. *Biochimie* **90**, 227-242
10. Kettritz, R. (2012) How anti-neutrophil cytoplasmic autoantibodies activate neutrophils. *Clin Exp Immunol* **169**, 220-228
11. Kessenbrock, K., Krumbholz, M., Schonermarck, U., Back, W., Gross, W. L., Werb, Z., Grone, H. J., Brinkmann, V., and Jenne, D. E. (2009) Netting neutrophils in autoimmune small-vessel vasculitis. *Nat Med* **15**, 623-625
12. Jerke, U., Hernandez, D. P., Beaudette, P., Korkmaz, B., Dittmar, G., and Kettritz, R. (2015) Neutrophil serine proteases exert proteolytic activity on endothelial cells. *Kidney Int* **88**, 764-775
13. Schreiber, A., Rousselle, A., Becker, J. U., von Massenhausen, A., Linkermann, A., and Kettritz, R. (2017) Necroptosis controls NET generation and mediates complement activation, endothelial damage, and autoimmune vasculitis. *Proc Natl Acad Sci U S A* **114**, E9618-E9625
14. Kallenberg, C. G. (2015) Pathogenesis and treatment of ANCA-associated vasculitides. *Clin Exp Rheumatol* **33**, S11-14
15. Yates, M., and Watts, R. (2017) ANCA-associated vasculitis. *Clin Med (Lond)* **17**, 60-64
16. Chaigne, B., and Guillevin, L. (2016) New therapeutic approaches for ANCA-associated vasculitides. *Presse Med* **45**, e171-178
17. Turk, D., Janjic, V., Stern, I., Podobnik, M., Lamba, D., Dahl, S. W., Lauritzen, C., Pedersen, J., Turk, V., and Turk, B. (2001) Structure of human dipeptidyl peptidase I (cathepsin C): exclusion domain added to an endopeptidase framework creates the machine for activation of granular serine proteases. *EMBO J* **20**, 6570-6582
18. Adkison, A. M., Raptis, S. Z., Kelley, D. G., and Pham, C. T. (2002) Dipeptidyl peptidase I activates neutrophil-derived serine proteases and regulates the development of acute experimental arthritis. *J Clin Invest* **109**, 363-371
19. Pham, C. T., Ivanovich, J. L., Raptis, S. Z., Zehnbauer, B., and Ley, T. J. (2004) Papillon-Lefevre syndrome: correlating the molecular, cellular, and clinical consequences of cathepsin C/dipeptidyl peptidase I deficiency in humans. *J Immunol* **173**, 7277-7281
20. Korkmaz, B., Lesner, A., Guarino, C., Wysocka, M., Kellenberger, C., Watier, H., Specks, U., Gauthier, F., and Jenne, D. E. (2016) Inhibitors and Antibody Fragments as Potential Anti-Inflammatory Therapeutics Targeting Neutrophil Proteinase 3 in Human Disease. *Pharmacol Rev* **68**, 603-630

21. Jenne, D. E., and Kuhl, A. (2006) Production and applications of recombinant proteinase 3, Wegener's autoantigen: problems and perspectives. *Clin Nephrol* **66**, 153-159
22. Dahl, S. W., Halkier, T., Lauritzen, C., Dolenc, I., Pedersen, J., Turk, V., and Turk, B. (2001) Human recombinant pro-dipeptidyl peptidase I (cathepsin C) can be activated by cathepsins L and S but not by autocatalytic processing. *Biochemistry* **40**, 1671-1678
23. Hamon, Y., Legowska, M., Herve, V., Dallet-Choisy, S., Marchand-Adam, S., Vanderlynden, L., Demonte, M., Williams, R., Scott, C. J., Si-Tahar, M., Heuze-Vourc'h, N., Lalmanach, G., Jenne, D. E., Lesner, A., Gauthier, F., and Korkmaz, B. (2016) Neutrophilic Cathepsin C Is Maturated by a Multistep Proteolytic Process and Secreted by Activated Cells during Inflammatory Lung Diseases. *J Biol Chem* **291**, 8486-8499
24. Molgaard, A., Arnau, J., Lauritzen, C., Larsen, S., Petersen, G., and Pedersen, J. (2007) The crystal structure of human dipeptidyl peptidase I (cathepsin C) in complex with the inhibitor Gly-Phe-CHN2. *Biochem J* **401**, 645-650
25. Hart, T. C., Hart, P. S., Bowden, D. W., Michalec, M. D., Callison, S. A., Walker, S. J., Zhang, Y., and Firatli, E. (1999) Mutations of the cathepsin C gene are responsible for Papillon-Lefevre syndrome. *J Med Genet* **36**, 881-887
26. Toomes, C., James, J., Wood, A. J., Wu, C. L., McCormick, D., Lench, N., Hewitt, C., Moynihan, L., Roberts, E., Woods, C. G., Markham, A., Wong, M., Widmer, R., Ghaffar, K. A., Pemberton, M., Hussein, I. R., Temtamy, S. A., Davies, R., Read, A. P., Sloan, P., Dixon, M. J., and Thakker, N. S. (1999) Loss-of-function mutations in the cathepsin C gene result in periodontal disease and palmoplantar keratosis. *Nat Genet* **23**, 421-424
27. Gorlin, R. J., Sedano, H., and Anderson, V. E. (1964) The Syndrome of Palmar-Plantar Hyperkeratosis and Premature Periodontal Destruction of the Teeth. A Clinical and Genetic Analysis of the Papillon-Lef'evre Syndrome. *J Pediatr* **65**, 895-908
28. Hart, T. C., and Shapira, L. (1994) Papillon-Lefevre syndrome. *Periodontol 2000* **6**, 88-100
29. Nagy, N., Valyi, P., Csoma, Z., Sulak, A., Tripolszki, K., Farkas, K., Paschali, E., Papp, F., Toth, L., Fabos, B., Kemeny, L., Nagy, K., and Szell, M. (2014) CTSC and Papillon-Lefevre syndrome: detection of recurrent mutations in Hungarian patients, a review of published variants and database update. *Mol Genet Genomic Med* **2**, 217-228
30. Hamon, Y., Legowska, M., Fergelot, P., Dallet-Choisy, S., Newell, L., Vanderlynden, L., Kord Valeshabad, A., Acrich, K., Kord, H., Charalampos, T., Morice-Picard, F., Surplice, I., Zoidakis, J., David, K., Vlahou, A., Ragunatha, S., Nagy, N., Farkas, K., Szell, M., Goizet, C., Schacher, B., Battino, M., Al Farraj Aldosari, A., Wang, X., Liu, Y., Marchand-Adam, S., Lesner, A., Kara, E., Korkmaz-Icoz, S., Moss, C., Eickholz, P., Taieb, A., Kavukcu, S., Jenne, D. E., Gauthier, F., and Korkmaz, B. (2016) Analysis of urinary cathepsin C for diagnosing Papillon-Lefevre syndrome. *FEBS J* **283**, 498-509
31. Roberts, H., White, P., Dias, I., McKaig, S., Veeramachaneni, R., Thakker, N., Grant, M., and Chapple, I. (2016) Characterization of neutrophil function in Papillon-Lefevre syndrome. *J Leukoc Biol* **100**, 433-444
32. Guarino, C., Hamon, Y., Croix, C., Lamort, A. S., Dallet-Choisy, S., Marchand-Adam, S., Lesner, A., Baranek, T., Viaud-Massuard, M. C., Lauritzen, C., Pedersen, J., Heuze-Vourc'h, N., Si-Tahar, M., Firatli, E., Jenne, D. E., Gauthier, F., Horwitz, M. S., Borregaard, N., and Korkmaz, B. (2017) Prolonged pharmacological inhibition of cathepsin C results in elimination of neutrophil serine proteases. *Biochem Pharmacol* **131**, 52-67
33. Perera, N. C., Wiesmuller, K. H., Larsen, M. T., Schacher, B., Eickholz, P., Borregaard, N., and Jenne, D. E. (2013) NSP4 is stored in azurophil granules and released by activated neutrophils as active endoprotease with restricted specificity. *J Immunol* **191**, 2700-2707
34. Sorensen, O. E., Clemmensen, S. N., Dahl, S. L., Ostergaard, O., Heegaard, N. H., Glenthoj, A., Nielsen, F. C., and Borregaard, N. (2014) Papillon-Lefevre syndrome patient reveals species-dependent requirements for neutrophil defenses. *J Clin Invest* **124**, 4539-4548
35. Korkmaz, B., Poutrain, P., Hazouard, E., de Monte, M., Attucci, S., and Gauthier, F. L. (2005) Competition between elastase and related proteases from human neutrophil for binding to alpha1-protease inhibitor. *Am J Respir Cell Mol Biol* **32**, 553-559

36. Halbwachs-Mecarelli, L., Bessou, G., Lesavre, P., Lopez, S., and Witko-Sarsat, V. (1995) Bimodal distribution of proteinase 3 (PR3) surface expression reflects a constitutive heterogeneity in the polymorphonuclear neutrophil pool. *FEBS Lett* **374**, 29-33
37. Schreiber, A., Busjahn, A., Luft, F. C., and Kettritz, R. (2003) Membrane expression of proteinase 3 is genetically determined. *J Am Soc Nephrol* **14**, 68-75
38. Korkmaz, B., Jaillet, J., Jourdan, M. L., Gauthier, A., Gauthier, F., and Attucci, S. (2009) Catalytic activity and inhibition of wegener antigen proteinase 3 on the cell surface of human polymorphonuclear neutrophils. *J Biol Chem* **284**, 19896-19902
39. Korkmaz, B., Lesner, A., Letast, S., Mahdi, Y. K., Jourdan, M. L., Dallet-Choisy, S., Marchand-Adam, S., Kellenberger, C., Viaud-Massuard, M. C., Jenne, D. E., and Gauthier, F. (2013) Neutrophil proteinase 3 and dipeptidyl peptidase I (cathepsin C) as pharmacological targets in granulomatosis with polyangiitis (Wegener granulomatosis). *Semin Immunopathol* **35**, 411-421
40. Schreiber, A., Otto, B., Ju, X., Zenke, M., Goebel, U., Luft, F. C., and Kettritz, R. (2005) Membrane proteinase 3 expression in patients with Wegener's granulomatosis and in human hematopoietic stem cell-derived neutrophils. *J Am Soc Nephrol* **16**, 2216-2224
41. Legowska, M., Hamon, Y., Wojtysiak, A., Grzywa, R., Sienczyk, M., Burster, T., Korkmaz, B., and Lesner, A. (2016) Development of the first internally-quenched fluorescent substrates of human cathepsin C: The application in the enzyme detection in biological samples. *Arch Biochem Biophys* **612**, 91-102
42. Guarino, C., Legowska, M., Epinette, C., Kellenberger, C., Dallet-Choisy, S., Sienczyk, M., Gabant, G., Cadene, M., Zoidakis, J., Vlahou, A., Wysocka, M., Marchand-Adam, S., Jenne, D. E., Lesner, A., Gauthier, F., and Korkmaz, B. (2014) New selective peptidyl di(chlorophenyl) phosphonate esters for visualizing and blocking neutrophil proteinase 3 in human diseases. *J Biol Chem* **289**, 31777-31791
43. Attucci, S., Korkmaz, B., Juliano, L., Hazouard, E., Girardin, C., Brillard-Bourdet, M., Rehault, S., Anthonioz, P., and Gauthier, F. (2002) Measurement of free and membrane-bound cathepsin G in human neutrophils using new sensitive fluorogenic substrates. *Biochem J* **366**, 965-970
44. Miller, S. A., Dykes, D. D., and Polesky, H. F. (1988) A simple salting out procedure for extracting DNA from human nucleated cells. *Nucleic Acids Res* **16**, 1215
45. Essawi, M., Gad, Y. Z., el-Rouby, O., Temtamy, S. A., Sabour, Y. A., and el-Awady, M. K. (1997) Molecular analysis of androgen resistance syndromes in Egyptian patients. *Dis Markers* **13**, 99-105
46. Selvaraju, V., Markandaya, M., Prasad, P. V., Sathyan, P., Sethuraman, G., Srivastava, S. C., Thakker, N., and Kumar, A. (2003) Mutation analysis of the cathepsin C gene in Indian families with Papillon-Lefevre syndrome. *BMC Med Genet* **4**, 5
47. Ragunatha, S., Ramesh, M., Anupama, P., Kapoor, M., and Bhat, M. (2015) Papillon-Lefevre syndrome with homozygous nonsense mutation of cathepsin C gene presenting with late-onset periodontitis. *Pediatr Dermatol* **32**, 292-294
48. Soliman, H., ELdeen, G. H., and Mustafa, I. M. (2015) A novel nonsense mutation in cathepsin C gene in an Egyptian patient presenting with Papillon–Lefèvre syndrome. *Egypt J Med Hum Genet* **16**, 387–392
49. Martinho, S., Levade, T., Fergelot, P., and Stephan, J. L. (2017) [Papillon-Lefevre syndrome: A new case]. *Arch Pediatr* **24**, 360-362
50. Bullon, P., Morillo, J. M., Thakker, N., Veeramachaneni, R., Quiles, J. L., Ramirez-Tortosa, M. C., Jaramillo, R., and Battino, M. (2014) Confirmation of oxidative stress and fatty acid disturbances in two further Papillon-Lefevre syndrome families with identification of a new mutation. *J Eur Acad Dermatol Venereol* **28**, 1049-1056
51. Jegot, G., Derache, C., Castella, S., Lahouassa, H., Pitois, E., Jourdan, M. L., Remold-O'Donnell, E., Kellenberger, C., Gauthier, F., and Korkmaz, B. (2011) A substrate-based approach to convert SerpinB1 into a specific inhibitor of proteinase 3, the Wegener's granulomatosis autoantigen. *FASEB J* **25**, 3019-3031

52. Dau, T., Sarker, R. S., Yildirim, A. O., Eickelberg, O., and Jenne, D. E. (2015) Autoprocessing of neutrophil elastase near its active site reduces the efficiency of natural and synthetic elastase inhibitors. *Nat Commun* **6**, 6722

FOOTNOTES

The abbreviations used are: α1PI, alpha-1-proteinase inhibitor; Ab, antibody; ABZ, *ortho*-aminobenzoic acid; ANCA, anti-neutrophil cytoplasmic autoantibody; BCA, bicinchoninic acid; Bt, biotin; CatC, cathepsin C; CG; cathepsin G; DMSO, dimethyl sulfoxide; ECL, enhanced chemiluminescence; EDDnp, *N*-(2.4-dinitrophenyl)ethylenediamine; FRET, fluorescence resonance energy transfer; GPA, granulomatosis with polyangiitis; HBSS, Hank's balanced salt buffer; HNE, human neutrophil elastase; HSC, hematopoietic stem cell; MPO, myeloperoxidase; NSP; neutrophil serine protease; PBS, phosphate-buffered saline; PEG, polyethlene glycol; PLS, Papillon-Lefèvre syndrome; PMN, polymorphonuclear neutrophil; PR3, proteinase 3; $PR3^{m}$, membrane-bound PR3; RT, room temperature; SDS-PAGE, sodium dodecyl sulfate polyacrylamide gel electrophoresis; WBC, white blood.

TABLE I
Patient's informations

Patients	Age (Years)	Gender	Ethnicity	CatC mutation	CatC activity	PR3 activity (%)
1	18	M	Indian *(India)*	c.912C>A (p.Y304X)[a] nonsense	Not detectable	4.3
2	12	F	Egyptian *(Egypte)*	c.711G>A (p.W237X)[b] nonsense	Not detectable	3.9*
3	8	F	Turkish *(France)*	c.628C>T (p.Arg210X)[c] c.1286G>A (p.Trp429X) Compound heterozygous nonsense	Not detectable	1.8
4	44	F	Italian *(Italy)*	c.1141delC (p.L381fsX393)[d] frameshift	Not detectable	1.8
5	20	M	Saudi Arabian *(Saudi Arabia)*	c.815G>C (p.R272P)[e] missense	Not detectable	2.1*
6	27	M	Saudi Arabian *(Saudi Arabia)*	c.815G>C (p.R272P)[e] missense	Not detectable	Not tested
7	5	M	Pakistanian *(UK)*	c.815G>C (p.R272P)[‡] missense	Not detectable	0.75
8	4	M	Pakistanian *(UK)*	c.815G>C (p.R272P)[‡] missense	Not detectable	1.8**
9	16	M	Pakistanian *(UK)*	c.815G>C (p.R272P)[‡] missense	Not detectable	0.63**
10	11	M	Pakistanian *(UK)*	c.815G>C (p.R272P)[‡] missense	Not detectable	0.50
11	16	F	Pakistanian *(UK)*	c.815G>C (p.R272P)[‡] missense	Not detectable	0.58**
12	14	M	British caucasian *(UK)*	c.415G>A (p.G139R)[‡] c.1280A>C (p.N427T) Compound heterozygous missense	Not detectable	0.50
13	17	F	Moroccan *(France)*	c.757G>A (p.A253I)[#] missense	Not detectable	1.7
14	11	M	Moroccan *(France)*	c.757G>A (p.A253I)[#] missense	Not detectable	2.0
15	13	F	Egyptian *(Egypte)*	Not identified	Not detectable	1.1**
16	7	M	Nubian[&] *(Egypte)*	c.1015C>T (p.R339C)[#] missense	Not detectable	0.8*
17	12	F	Nubian *(Egypte)*	c.1015C>T (p.R339C) *suspected*	Not detectable	0.9*
18	12	M	Egyptian *(Egypte)*	Not identified	Not detectable	1.3*
19	12	M	Egyptian *(Egypte)*	a splice site mutation in intron **3** IVS3-1G → A	Not detectable	1.5*
20	17	M	Egyptian *(Egypte)*	Not identified	Not detectable	2.1
21	13	M	Egyptian *(Egypte)*	Not identified	Not detectable	2.5

[#]CatC mutations identified in this work. [‡]Identified by Professor N.S Thakkar, Academic Unit of Medical Genetics, University of Manchester, Manchester, UK. The mutation carried by patients 13 and 14 were determined as in Hamon *et al.*, 2016 (30)

[a] Ragunatha *et al.*, 2015 (47)

[b] Soliman *et al.,* 2015 (48)
[c] Martinho *et al.*, 2017 (49)
[d] Bullon *et al.*, 2014 (50)
[e] Hamon *et al.,* 2016 (30)

Patient 13 and patient 14 are siblings
Patient 16 and patient 17 are siblings
Patient 2 and patient 15 are cousins

* Purified neutrophil lysates
** WBC lysates
[&] The Nubian ethnicity people are also North African (residing upper Egypt at the borders with Sudan) but they have characteristic features of dark skin and African facial features.

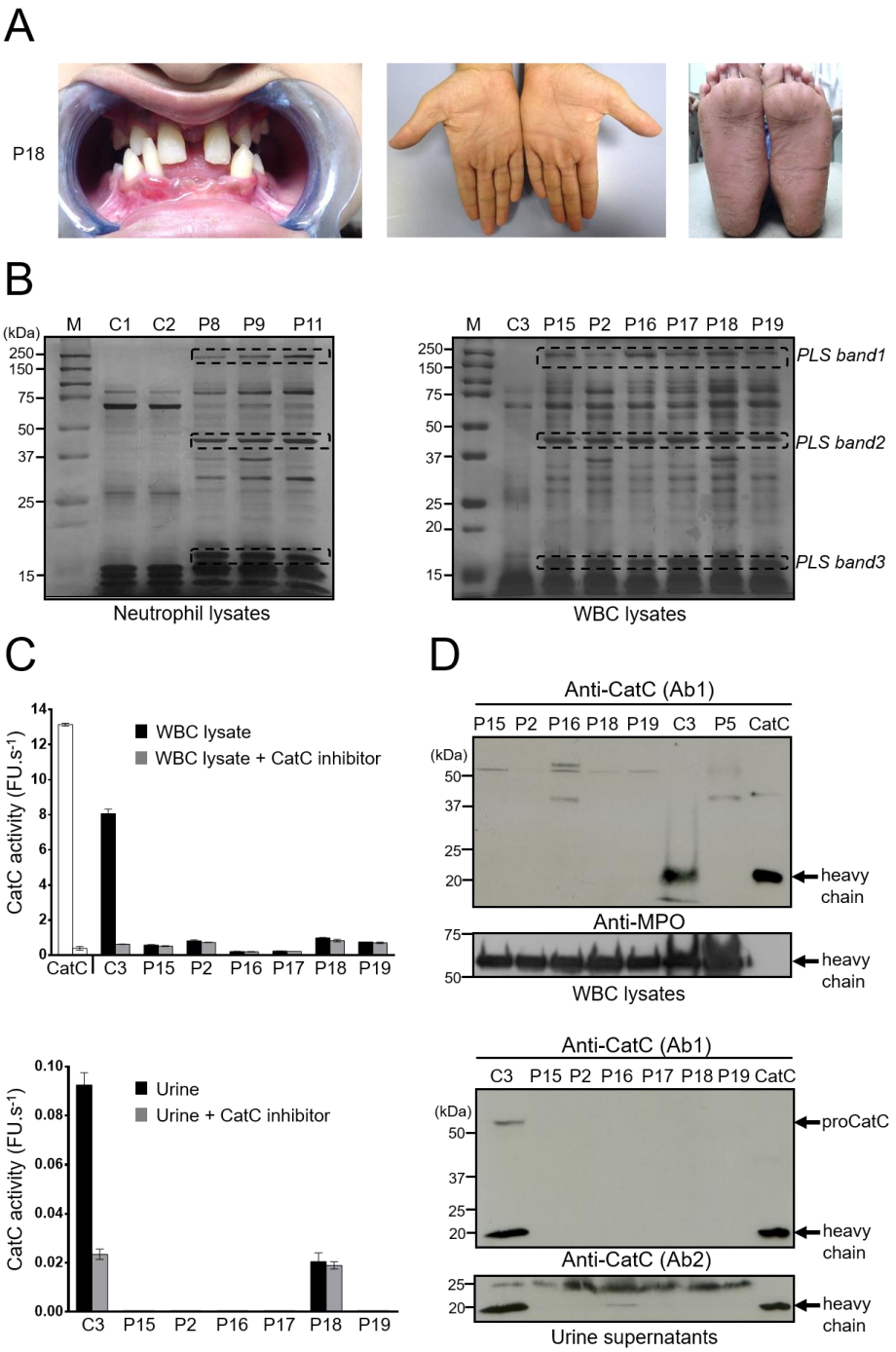

Figure 1. CatC in biological samples of PLS patients. (A) Characteristic dental and palmoplantar features of PLS (patient 18). Photos show early loss of teeth and hyperkeratosis of the palms and soles. (B) Neutrophil and WBC lysates from PLS patients and from healthy controls, lysed in 50 mM HEPES buffer, 750 mM NaCl, 0.05% NP40, pH 7.4 during 5 min at RT and analyzed by SDS-PAGE (12%) /silver staining under reducing conditions (10 µg/lane) strongly differ by their protein profile. (C) Measurement of CatC activity in WBC lysates (10 µg of protein) (*Top*) and concentrated urines (*Bottom*) in the presence or not of a selective CatC inhibitor. The residual proteolytic activity was not inhibited by the CatC inhibitor which demonstrates the absence of CatC activity in PLS samples. (D) Western-blot analysis of WBC lysates (10 µg of protein) and concentrated urines of PLS samples and controls using anti-CatC antibodies shows the absence of the CatC heavy chain in all PLS samples. The urines were collected and analyzed as in Hamon *et al.*, 2016 (30). C: control, P: PLS patient, FU: fluorescence unit.

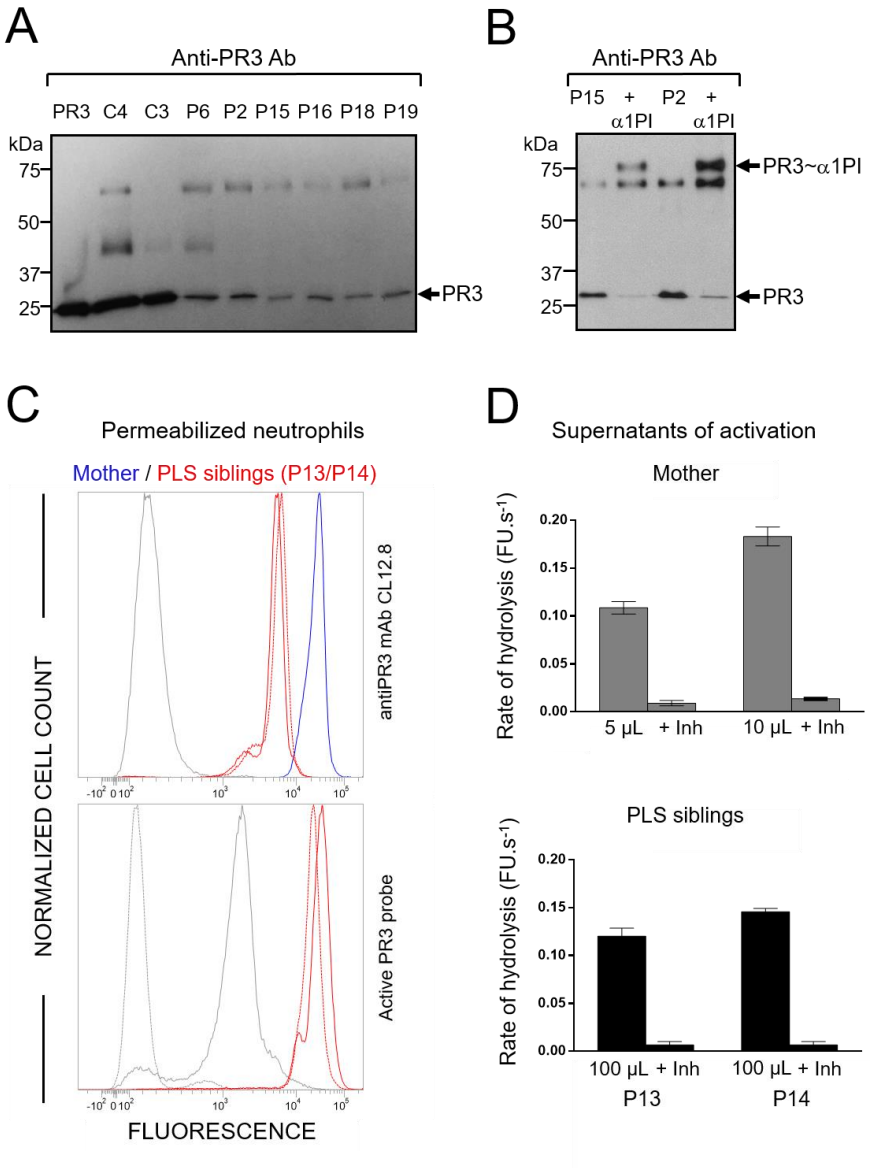

Figure 2. Active PR3 in PLS blood samples. (A) Western-blotting of WBC lysates (10 µg of protein) from PLS and healthy controls using anti-PR3 antibodies: low amounts of PR3 are present in PLS samples. (B) Western-blotting of PLS white blood cells lysates (10 µg of protein) incubated with α1PI (5 µM) in 50 mM HEPES buffer, 750 mM NaCl, 0.05% NP40, pH 7.4 during 3 h at 37°C. The de novo formation of irreversible α1PI-PR3 complexes of about 75 kDa reveals that PR3 is proteolytically active in spite of the absence of active CatC. (C) (*Top*) Flow cytometry analysis of the expression of PR3 in permeabilized PLS neutrophils. Using anti-PR3 antibodies, a lesser fluorescence is observed in permeabilized neutrophils from two PLS siblings (P13 and P14) (red) as compared with their mother used here as a control (blue). The grey peak corresponds to the isotype control. (*Bottom*). The use of PR3 activity probe Biotin-PEG_{66}-PYDA(O-C_6H_4-4-Cl)$_2$ as in Guarino *et al*., (42) shows that the residual PLS PR3 is enzymatically active. The gray peek indicates the fluorescence of permeabilized neutrophils incubated with streptavidin-Alexa Fluor®488. The dotted gray peak corresponds to the (auto)fluorescence of permeabilized neutrophils. (D) PR3 activity in supernatants of calcium ionophore A23187 (Sigma-Aldrich, St. Quentin Fallavier, France) activated WBC in the presence or absence of the specific PR3 inhibitor Ac-PYDA(O-C_6H_4-4-Cl)$_2$. PR3 activity in PLS cell supernatants is about 1/20 of that in control cells and is almost totally inhibited in the presence of the selective PR3 inhibitor. C: control, Inh: inhibitor, P: PLS patient, FU: fluorescence unit.

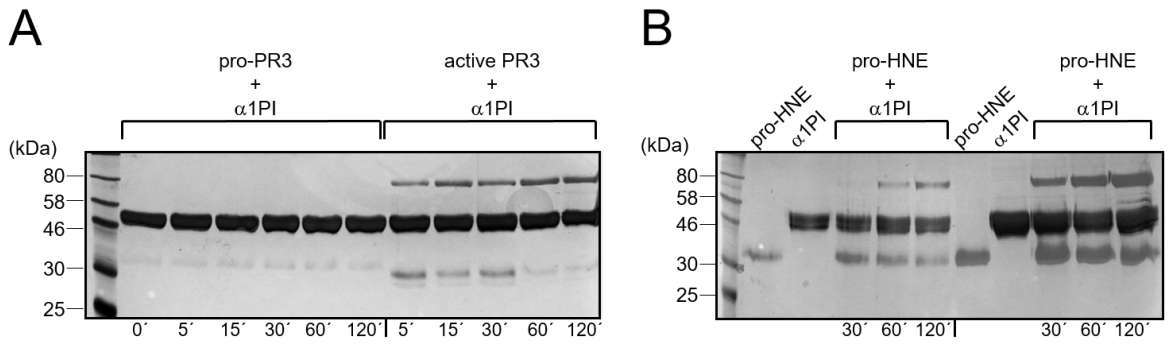

Figure 3. Irreversible complex formation analysis of pro-PR3 and pro-HNE with α1PI. (A) Recombinant pro-PR3 (0.8 µM), mature PR3 (0.8 µM) produced and purified as in (51) and (B) pro-HNE (1 µM), HNE (3 µM) produced and purified as in (52) were incubated with recombinant α1PI (5 µM) in 50 mM HEPES buffer, 750 mM NaCl, 0.05% NP40, pH 7.4 at 37°C, and then analyzed by SDS-PAGE and silver staining. The formation of stable covalent complexes of about 75 kDa was observed with pro-HNE but not with pro-PR3 as visualized in 15% SDS-PAGE under reducing and denaturing conditions.

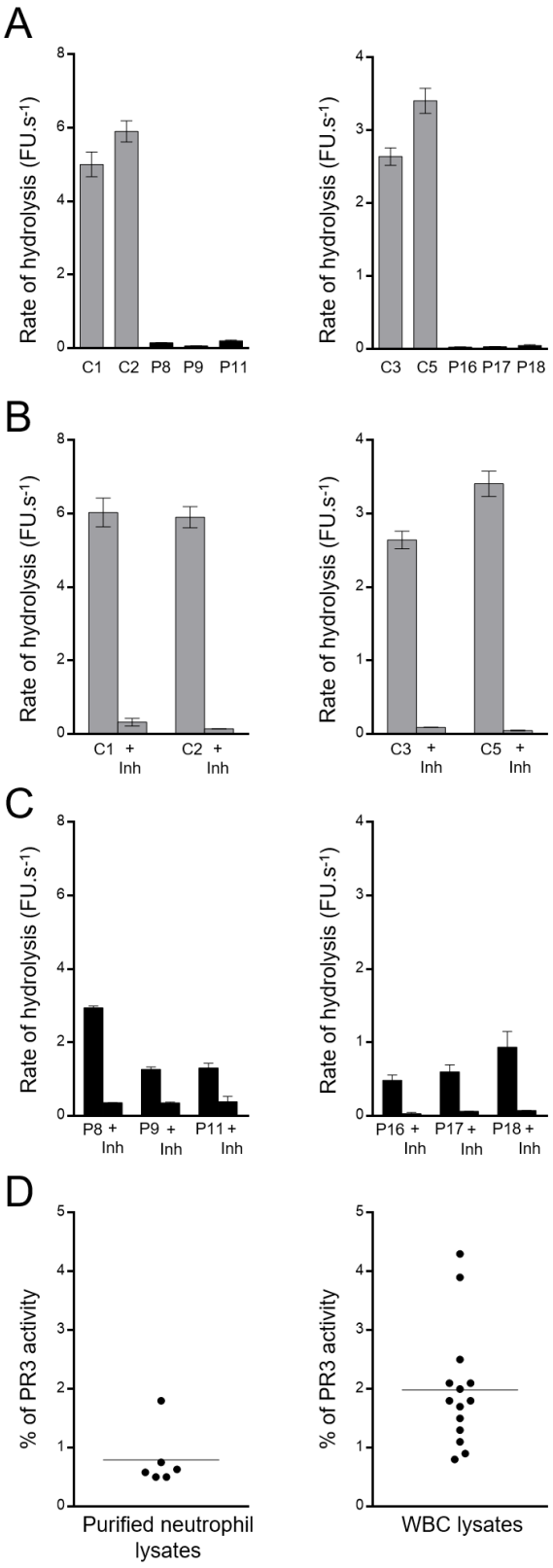

Figure 4. PR3 activity in PLS blood samples. PR3 activities in purified neutrophil (A, *Left*) or in WBC lysates (A, *Right*). PR3 activities were measured with the selective substrate ABZ-VAD(nor)VADYQ-EDDnp. Samples were also incubated with the selective PR3 inhibitor Bt-PYDA(O-C_6H_4-4-Cl)$_2$ to distinguish PR3 activity and nonspecific signal (B,C). Low levels of active PR3 were found in PLS cell lysates (5µg) compared to control cell lysates (0,25µg). (D) Percentage of PR3 activity in neutrophils and whole blood samples. We calculated the percentage of PR3 activity in purified neutrophils and in WBC of PLS patients (n=20) compared to healthy controls cells (n=11). We estimated that PLS cells contained 0.5 to 4 % of PR3 activities compared to healthy cells. Similar results were found in three independent experiments. C: control, Inh: inhibitor, P: PLS patient, FU: fluorescence unit.

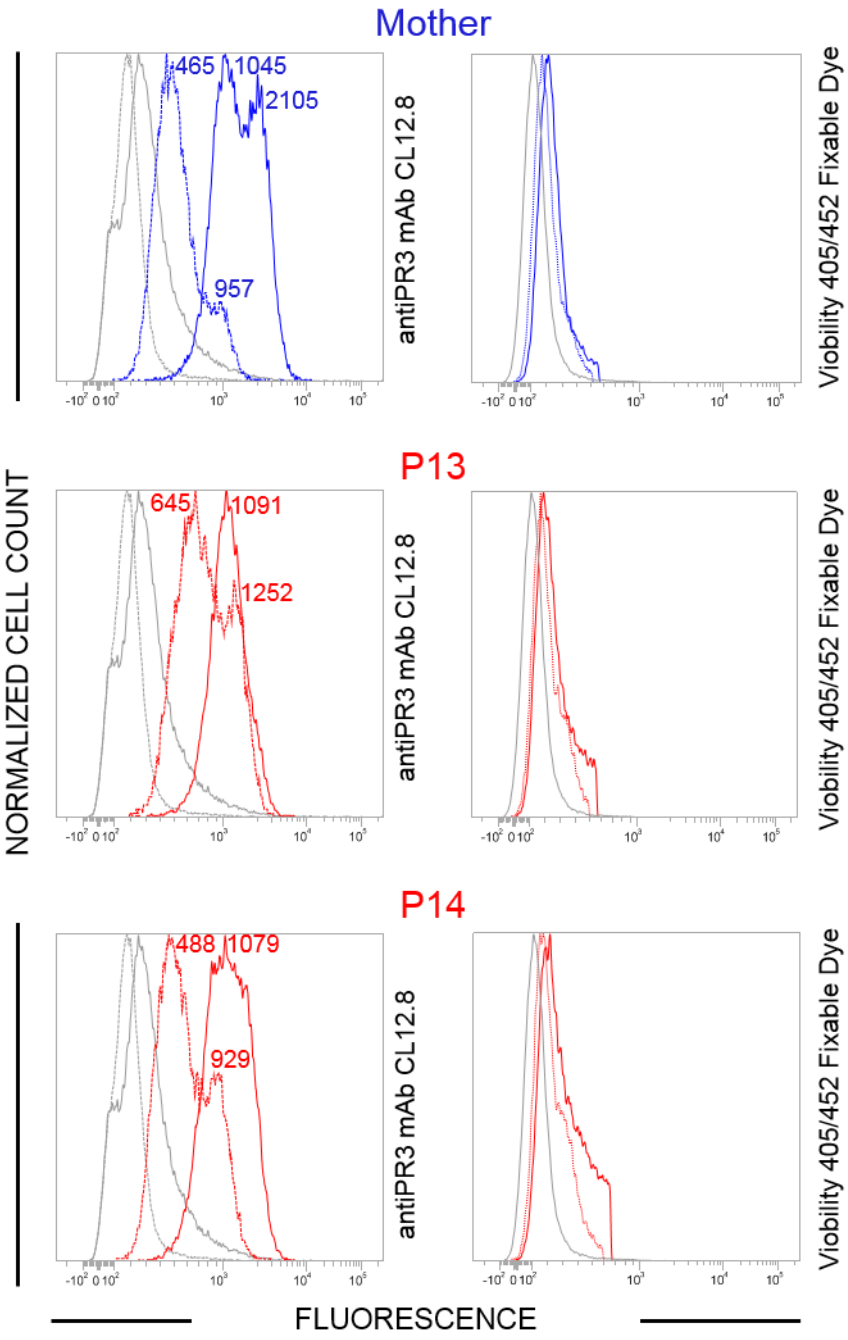

Figure 5. Membrane expression of PR3 on quiescent and chemically activated PLS neutrophils. WBC from PLS siblings (local patients P13 and P14) and their mother were activated using calcium ionophore (A23187) 30 min after blood collection. Both viable quiescent PLS (red dotted line) and control (blue dotted line) cells showed expression of PR3 on their surface. After chemical activation (continuous lines), membrane PR3 was largely increased on control cells while PR3 on PLS neutrophils was almost the same as on quiescent cells. We used Viobility 405/452 Fixable Dye to discriminate between live and apoptotic/dead cells. Flow cytometry revealed 81±5% viable neutrophils in all samples. No statistically significant difference between quiescent and activated neutrophils was observed (*t* test). P: PLS patient. Numbers indicate mean fluorescent intensity values.

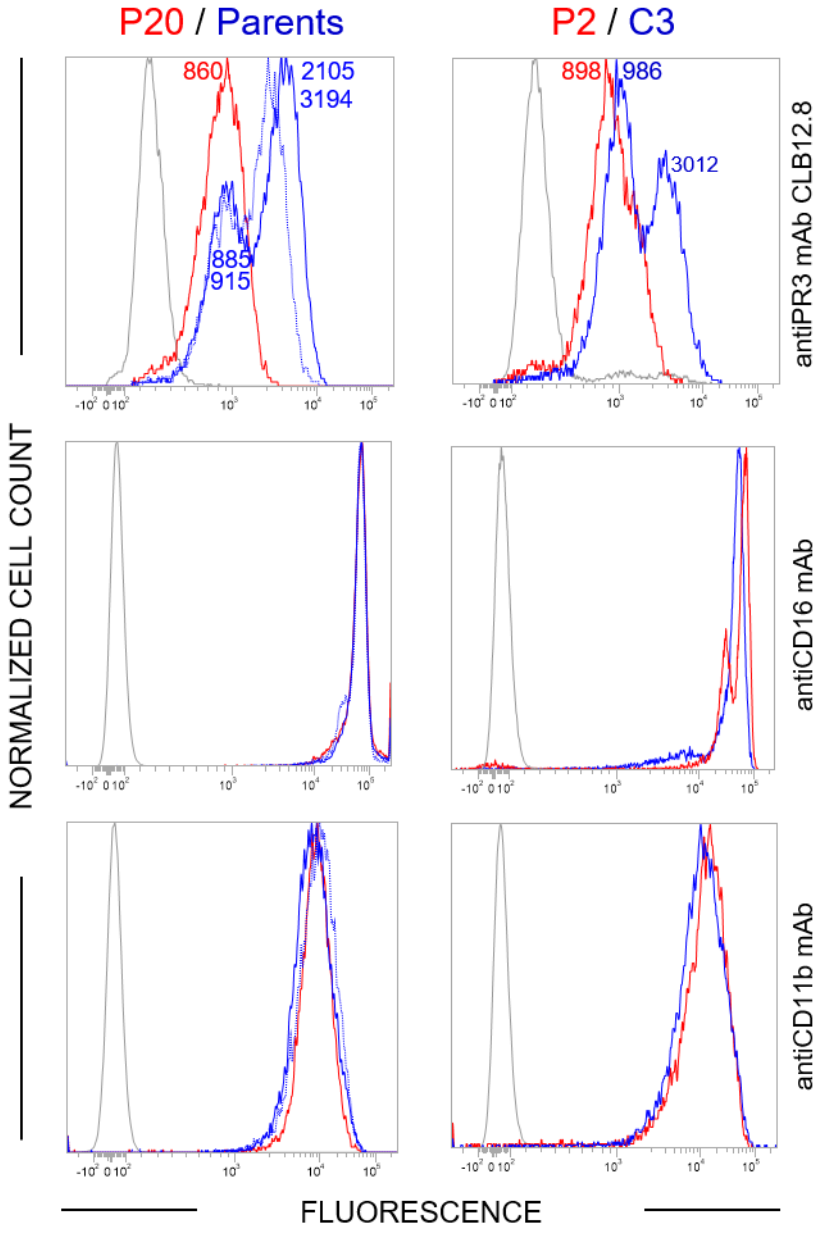

Figure 6. Membrane expression of PR3 on PLS neutrophils activated during transportation. PR3 expression on spontaneously activated neutrophils was investigated by flow cytometry. Control of cell activation was made using an anti-CD16 and an anti-CD11b antibody. Control cells were from parents or from randomly selected blood donors in the local environment of the patient. C: control, P: PLS patient. Similar results were obtained with cells from 9 other PLS patients.

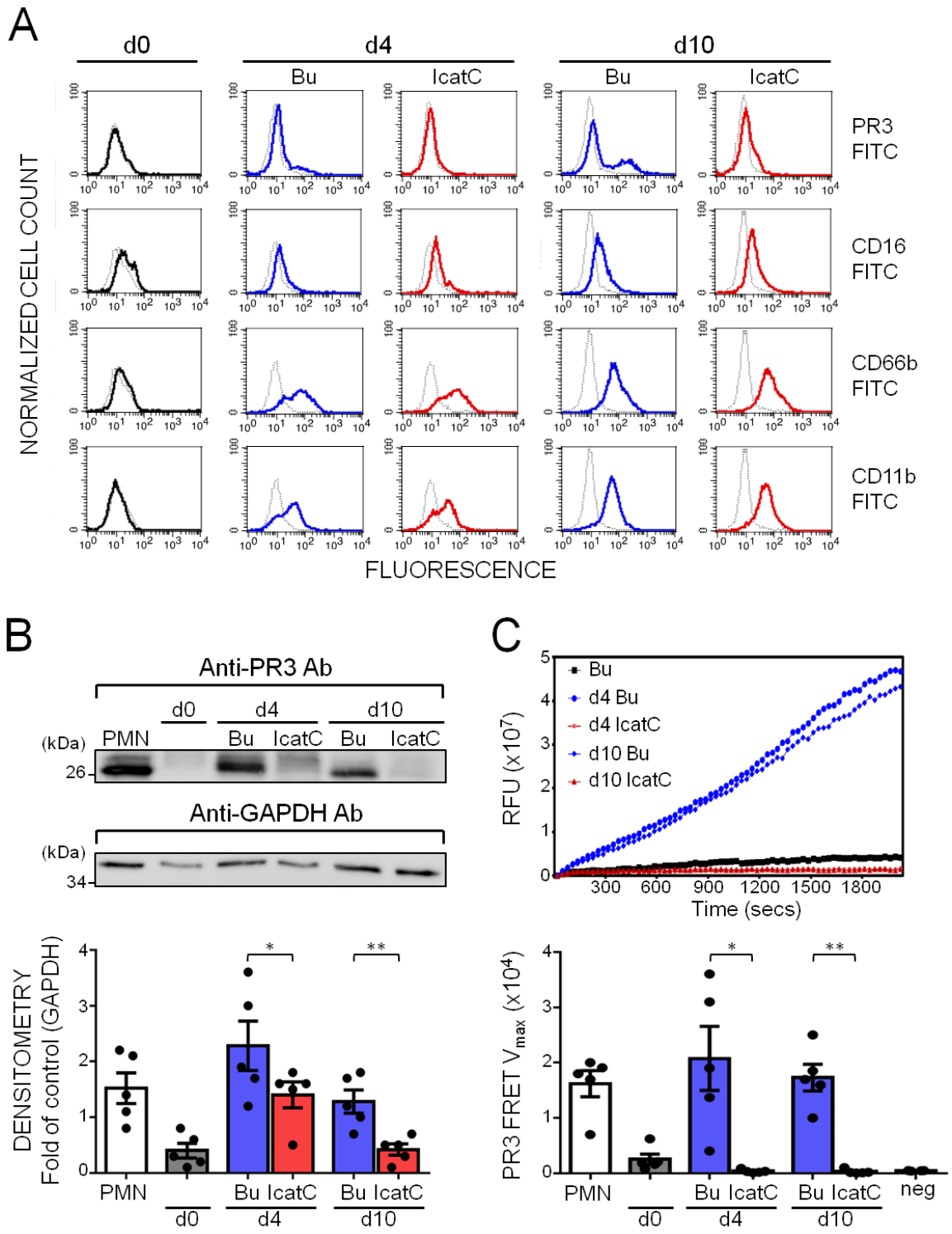

Figure 7. Effect of pharmacological CatC inhibition on PR3 expression and proteolytic activity in neutrophil-differentiated CD34⁺ HSC. CD34⁺ HSC were differentiated over 10 days into neutrophils in the presence of DMSO buffer control (Bu, blue) or 1 µM of the CatC inhibitor (IcatC, red). (A) Flow cytometry indicates that differentiating cells acquired the typical neutrophil surface markers CD16, CD66b, and CD11b, together with a bimodal membrane PR3 phenotype. Color lines represent staining with the specific antibodies and dotted lines represent the corresponding isotype control. A representative of five independent differentiation experiments is shown. (B) PR3 protein was assessed in cell lysates (7.0 µg/lane) by immunoblotting at the indicated time points using a specific anti-PR3 antibody. PR3 protein was strongly induced during CD34⁺ HSC differentiation and this effect was significantly reduced with IcatC. A representative western blot and the densitometric analysis from five

independent differentiation experiments is shown. *Bars* indicate mean ± SEM value of each condition and asterisks the p-value of *t* test ($p < 0.05$, *; $p < 0.01$, **). (C) Proteolytic PR3 activity was assessed in cell lysates (2.5 µg protein) at the indicated time points using the PR3-specific FRET substrate ABZ-VAD(nor)VADYQ-EDDnp. Representative PR3 substrate conversion curves from one of five independent differentiation experiments are depicted together with the corresponding statistics for the mean Vmax values ± SEM (n=5 independent differentiation experiments). The data show a complete loss of proteolytic PR3 activity with CatC inhibition. Isolated normal blood neutrophils (PMN) served as a positive and endothelial cell line as a negative control (neg ctrl). Asterisks indicate the p-value of *t* test ($p < 0.05$, *; $p < 0.01$, **).

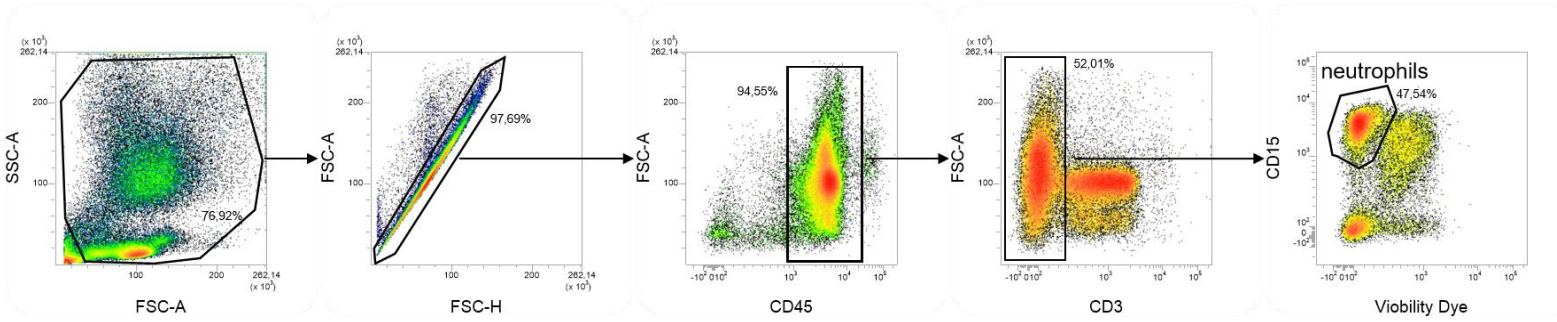

Supp.Figure 1. Gating strategies. WBC were isolated from EDTA-whole blood by red blood cells lysis. T cells and dead cells were excluded using anti-CD3 Ab and Viobility 405/520 Fixable Dye. The remaining cells were analyzed for the expression of CD15, a neutrophil marker. The percentages of cells in each of the specified gates are indicated.

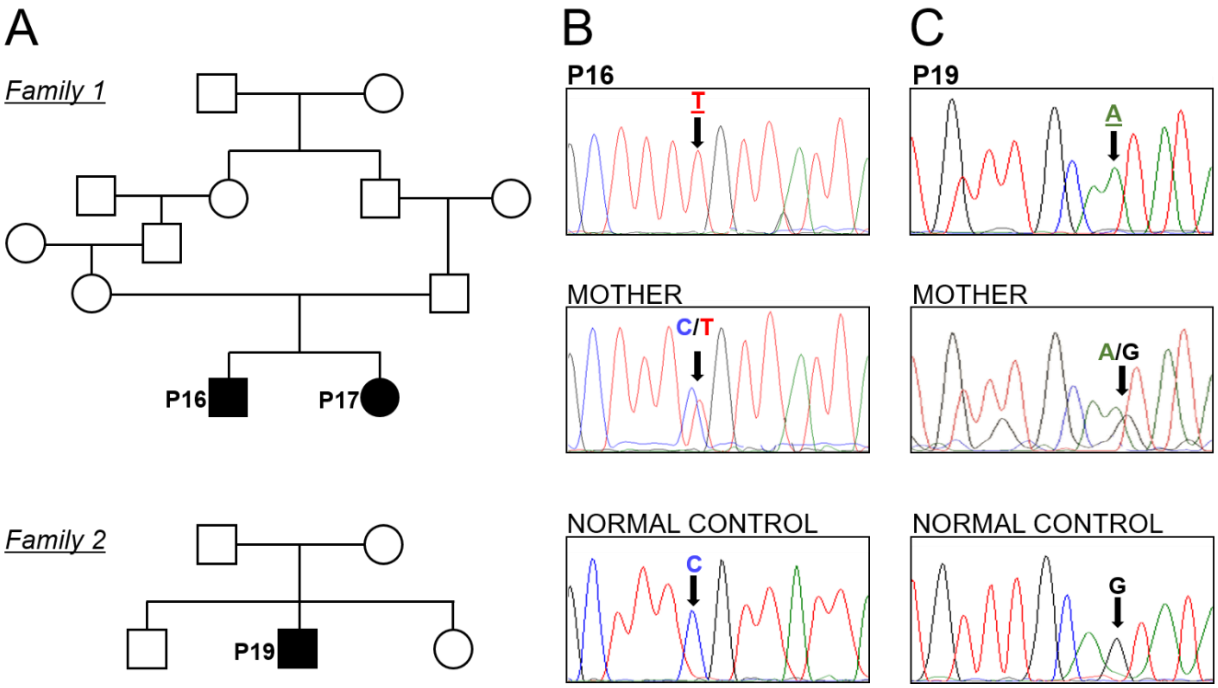

Supp.Figure 2. Pedigrees and genetic analysis of PLS patients. (A) Pedigree chart for family 1 and family 2. Multigenerational pedigree of family 1 showing two affected siblings (P16 and P17) of consanguineous parents. Family tree 2 shows one affected son of consanguineous parents. (B) *CTSC* gene exon 7a sequence, the upper chromatogram showing the homozygous missense mutation 1015C→T (R339C) in patient 16 (P16), the middle chromatogram shows the heterozygous mutation of the healthy mother and the lower chromatogram shows the normal sequence of a unrelated individual. (C) CTSC gene exon 3 sequence. DNA sequence of exon 3 showing the homozygous missense mutation 1015C→T (R339C) in patient 19 (P19), the middle chromatogram shows the heterozygous genotype of the healthy mother and the lower chromatogram shows the normal sequence of an unrelated individual.

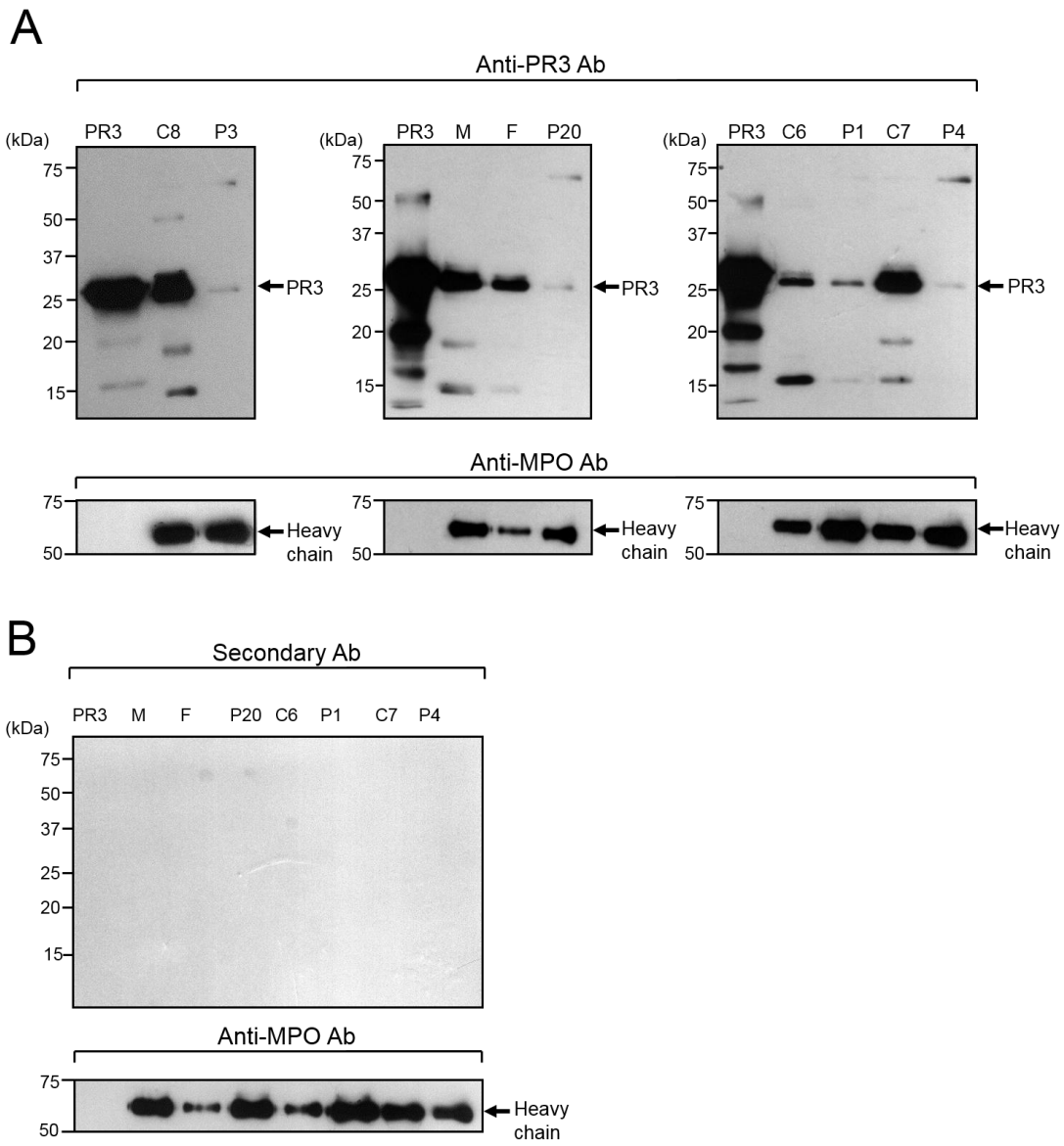

Supp.Figure 3. PR3 in PLS blood samples. (A) Western-blotting of WBC lysates (10 µg of protein) from PLS and healthy controls using a primary anti-PR3 Ab and a secondary HRP-labelled Ab. Amounts of PR3 were found to be highly reduced in PLS cells compared to healthy controls or parents. (B) Western-blotting of WBC lysates (10 µg of protein) from PLS and healthy controls developed with the HRP-labelled secondary antibody. No unspecific Ab binding was observed. We used an anti-MPO antibody as a positive control for the unaltered levels of MPO. C: control, P: PLS patient, M: mother, F, father.

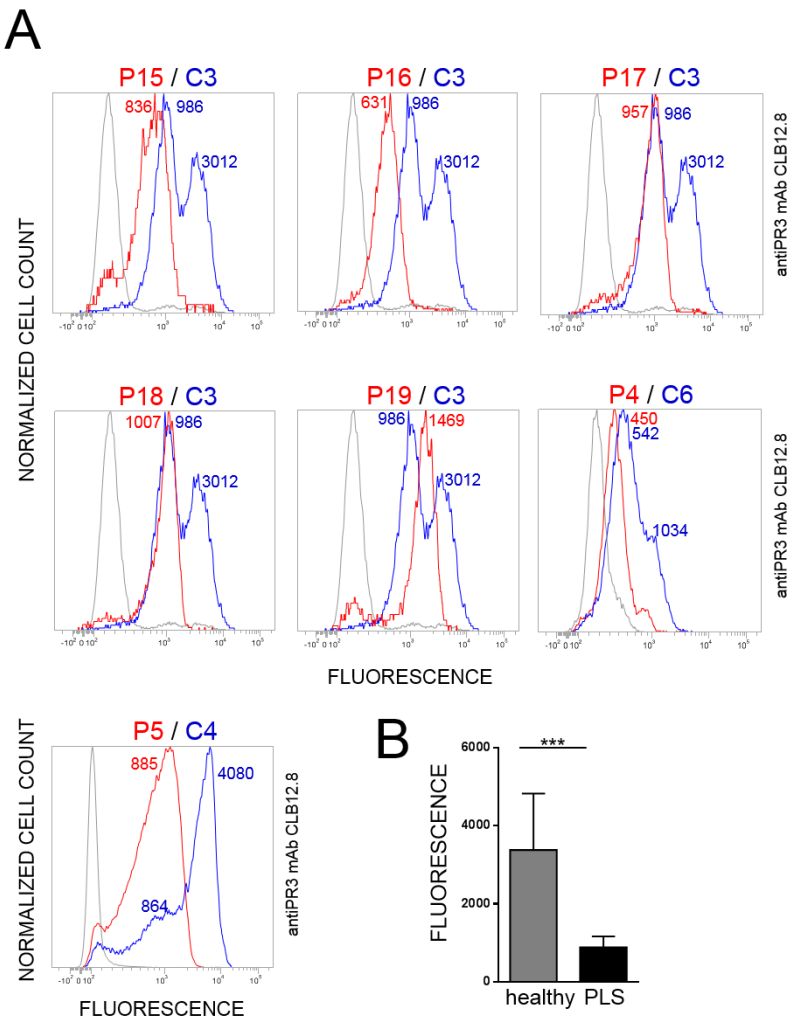

Supp.Figure 4. Membrane expression of PR3 on PLS neutrophils activated during transportation. (A) PR3 expression on spontaneously activated neutrophils was investigated by flow cytometry. Controls were randomly selected in the local environment of the patient. (B) Mean fluorescence intensity values for $PR3^{m}$ on PLS and healthy neutrophils. Bar indicates mean ± SEM value of each condition and asterisks the p-value of *t* test ($p< 0.001$,***). C: control (n=3), P: PLS patient (n=7).